Appendix 3

MICROBIAL DIVERSITY AND PRODUCTIVITY OF JINATA ONSEN, AN IRON-RICH INTERTIDAL HOT SPRING IN JAPAN

Lewis M. Ward, Airi Idai, Woodward W. Fischer, and Shawn E. McGlynn. In preparation.

Abstract

The redox history of Earth's atmosphere and oceans has varied dynamically through time, profoundly impacted by and in turn impacting life. The fluid Earth today is well oxygenated thanks to oxygenic photosynthesis by plants, algae, and Cyanobacteria, yet this state of affairs is unique to the Phanerozoic. Throughout the Proterozoic, the atmosphere contained at least some free oxygen while much of the oceans remained anoxic with varying amounts of free sulfide and ferrous iron. The interactions between these redox-active compounds and their role in biological productivity is not well constrained, partially as a result of the lack of appropriate process analogs for investigating the diversity and productivity of microorganisms supported by a range of combinations of free oxygen, iron, and sulfur compounds.

Hydrothermal environments, including terrestrial hot springs and near-shore hydrothermal vents, can contain diverse geochemical conditions that vary over short spatial scales thanks to the interactions between the oxygenated atmosphere, reducing hydrothermal fluids, and in some cases seawater.

One such process analog environment occurs at Jinata Onsen, on Shikinejima Island, Japan, where an intertidal, anoxic, iron- and hydrogen-rich hot spring mixes with

the oxygenated atmosphere and sulfate-rich seawater over short spatial scales, creating an enormous range of redox environments. Particular locations along the spring outflow support microbial communities and precipitated mineral textures potentially analogous to a range of early Earth environments, despite being separated by no more than a few meters.

Here, we characterize the geochemical conditions along the outflow of Jinata Onsen, as well as characterization of the microbial communities present via 16S amplicon metagenomic sequencing. Near the hot spring source, productivity is driven by oxidation of molecular hydrogen and ferrous iron by members of the Aquificales and Zetaproteobacteria, respectively, while downstream the microbial community transitions to being dominated by oxygenic Cyanobacteria. Cyanobacteria abundance and productivity dominates even at ferrous iron concentrations up to ~150 μM, challenging previous hypotheses of iron toxicity as a limitation to cyanobacterial expansion in the Precambrian ocean.

Background

Throughout Earth history, the metabolic opportunities available to life, and the resulting organisms and metabolisms responsible for driving primary productivity, have been shaped by the geochemical conditions of the atmosphere and oceans. Over the course of Earth's 4.56 billion year history, the redox state and overall geochemical conditions of the oceans have varied tremendously. The modern, sulfate-rich, well-oxygenated ocean that we see today is a relatively recent state, typical only of only the last few hundred million years (e.g. Lyons et al. 2014). For the first half of Earth history, until ~2.3 billion years ago (Gya), the atmosphere and oceans were anoxic (Johnson et al. 2014), and the oceans were

largely rich in dissolved iron but poor in sulfur (Walker and Brimblecombe 1985). Following the Great Oxygenation Event ~2.3 Gya, the atmosphere and surface ocean accumulated some oxygen, and the ocean transitioned into a stratified state with oxygenated surface waters and anoxic deeper waters, rich in either dissolved iron or sulfide (Poulton et al. 2010). This stratified ocean, though possibly variable, largely persisted for 1.5 billion years until the Neoproterozoic Oxygenation Event led to the ventilation of the deep oceans and the development of relatively modern ocean conditions (Sahoo et al. 2012). It is only under modern, well-oxygenated ocean conditions that Earth has supported the development of complex multicellular organisms like animals (Catling et al. 2005), and the biosphere was almost exclusively microbial throughout the earlier shifts in ocean chemistry.

As ocean conditions changed through the Archean and Proterozoic, the metabolic opportunities available to life also changed. The accumulation of oxygen enabled aerobic respiration and oxygen-fueled geochemical cycling of compounds like nitrogen and sulfur, while the abundance of compounds like ferrous iron and sulfide determined the potential productivity of anoxygenic phototrophs and lithotrophs. While we can gain some insight into the response of the biosphere to shifting ocean conditions over the course of Earth history by interpreting geochemical signatures in the rock record (e.g. the nitrogen isotope record of the evolution of the biogeochemical nitrogen cycle, Zerkle et al. 2017), an independent, complementary approach is to observe the activity of natural microbial communities in process analog environments which reflect some characteristics of ancient Earth environments. Many individual environments have been characterized that are

interpreted to be analogous to a particular period in Earth history; these include Lake Matano, in Indonesia, interpreted as being analogous to the ferruginous ocean (Crowe et al. 2008), Oku-Okuhachikurou Onsen in Akita Prefecture, Japan, similar to conditions just following the GOE (Ward et al. 2017), and the Black Sea, analogous to the stratified, anoxic- and sulfidic-at depth Proterozoic ocean (Scott et al. 2008). These analogs are each valuable in their own right, but the major differences between context at each site makes it difficult to isolate individual variables that lead to shifts in microbial community and productivity. An ideal test case for understanding the shifts of microbial productivity over the course of Earth history would be a system in which conditions of oxygen concentration and abundance of compounds such as sulfur and iron vary over short spatial scales under otherwise similar conditions. One such system occurs at Jinata Onsen, on Shikinejima Island, Tokyo Prefecture, Japan. At Jinata, an iron-rich hot spring emerges near a small bay, and mixes with seawater over the course of a few meters, quickly transitioning from an iron-rich and oxygen-poor condition, analogous to some conditions in the early Proterozoic, toward iron-poor and sulfate- and oxygen-rich conditions typical of the modern open ocean. Here, we characterize the geochemistry of this hot spring and describe the microbial community along the hot spring outflow as it mixes with ocean water via culture-independent 16S amplicon metagenomic sequencing. We show that the microbial community shifts from being dominated by iron- and hydrogen-oxidizing bacteria toward Cyanobacteria downstream. Furthermore, we show that Cyanobacteria become abundant even at high (>100 μM) Fe^{2+} concentrations, challenging interpretations of iron toxicity determining cyanobacterial ecology early in Earth history. Furthermore, we identify novel

high-temperature lineages of a number of microbial taxa, including iron-oxidizing Zetaproteobacteria.

Materials and Methods:

Geological context and sedimentology of Jinata:

Jinata Onsen is located at approximately 34.318N, 139.216E on the island of Shikinejima, Tokyo Prefecture, Japan. Shikinejima is part of the Izu Islands, a chain of volcanic islands which formed in the last few million years along the northern edge of the Izu-Bonin-Mariana Arc (Kaneoka et al. 1970). Shikinejima is formed of Late Paleopleistocene- to-Holocene non-alkaline felsic volcanics and Late-Miocene to Pleistocene non-alkaline pyroclastic volcanic flows (Figure 1).

The source water of Jinata Onsen emerges anoxic, iron-rich, and gently bubbling from the spring source (Figure 2). Temperatures at the source are ~62°C. Water emerges into the Source Pool, which has no visible microbial mat or biofilms. Surfaces are instead coated with a fluffy red precipitate, likely a poorly-ordered iron oxide phase such as ferrihydrite. The Source Pool has no mixing with seawater. Downstream, the spring water collects into a series of pools (Pool 1-3), which sequentially cool. Pool 1 is dominated by precipitated iron oxides, like the Source Pool, but also contains what appear to be microbial streamers that are mineralized and coated in iron oxides. Downstream pools (Pools 2 and 3) also mix with seawater during high tide. Samples were collected and temperatures were measured at high tide, reflecting the lowest temperatures experienced by microbes in the pools—at low

tide, hot spring input is dominant and temperatures rise. Surfaces in Pools 2 and 3 are covered in thick microbial mats. In Pool 2, the mat is coated in a layer of fluffy iron oxide similar to that in the source pool, with dense microbial mat below. Pool 3 contains only patchy iron oxides, with mostly exposed microbial mats displaying a finger-like morphology, potentially related to turbulent mixing during high tide. The Outflow is the outlet of a channel connecting Pool 2 to the bay. It is dominantly marine with a constant flow of spring water.

Sample collections:

Samples were collected from 5 sites at Jinata Onsen: the Source Pool, Pool 1, Pool 2, Pool 3, and the Outflow. Two samples were collected per site. At the Source Pool, Sample A was taken from the top of a ~10cm cobble and Sample B was collected from the bottom. In Pool 1, Sample A was taken of the yellow precipitate deeper in the pool, while Sample B was the redder, shallower section with abundant streamer-like structures. Pool 2 Sample A was an orange-ish mat collected from the side of a boulder. Pool 2 Sample B was a more cohesive greenish mat. Pool 3 Sample A was one of the finger-like mat structures. Sample B was a mottled, rough orange-green mat sample. At the Outflow, Sample A was taken from within the stream exiting Pool 2, while Sample B was taken of a mat within the swash zone.

Samples were collected as mineral scrapings of floc-y iron oxides upstream (Source Pool and Pool 1) and as samples of microbial mat downstream (Pools 2 and 3, and Outflow) using sterile forceps and spatulas (~0.25 cm^3 of material). Cells were lysed and DNA preserved in the field using a Zymo Terralyzer BashingBead Matrix and Xpedition

Lysis Buffer. Cells were disrupted immediately by attaching tubes to the blade of a cordless reciprocating saw and operating for 1 minute. Samples for geochemical analysis consisted of water collected via sterile syringe and filtered immediately through a 0.2 micron filter and gas bubbles collected from the source pool via funnel and sterile syringe and injected immediately into an anoxic serum vial to positive pressure.

Geochemical analysis:

Dissolved oxygen (DO), pH, and temperature measurements were performed *in situ* using an Exetech DO700 8-in-1 Portable Dissolved Oxygen Meter. Iron concentrations were measured using the ferrozine assay (Stookey 1970) following acidification with 40 mM sulfamic acid to inhibit iron oxidation by O_2 or oxidized nitrogen species (Klueglein and Kappler 2013). Ammonia/ammonium concentrations were measured using a TetraTest NH_3/NH_4^+ Kit with a Thermo Scientific Nanodrop 2000c spectrophotometer. Anion concentrations were measured via ion chromatography on a Shimadzu Ion Chromatograph equipped with a Shodex SI-90 4E anion column. Gas content of bubbles was determined via Shimadzu GC-14A gas chromatograph.

Microscopy.

Light microscopy images (Figure 4) were taken on a Zeiss Axio Imagers 2 Upright microscope (Zeiss, Germany) with 40 and 100x objective lens. Fluorescent images of DAPI (4=,6-diamidino-2-phenylindole)-stained samples were taken with an excitation wavelength below 395 nm and an emission wavelength between 420 and 470 nm. The autofluorescence of Cyanobacteria was detected by exposing the sample to a wavelength of between 395 and 440 nm and detecting the emission at a wavelength of 470 nm. Images of

DAPI fluorescence and autofluorescence were overlain using the FIJI software package (http://pacific.mpi-cbg.de).

Sequencing and analysis:

Following return to the lab, DNA was purified with a Zymo Soil/Fecal DNA extraction kit (Zymo Research, Irvine, CA). The V4-V5 region of the 16S rRNA gene was amplified from each extract as well as negative controls using archaeal and bacterial primers 515F (GTGCCAGCMGCCGCGGTAA) and 926R (CCGYCAATTYMTTTRAGTTT) (Caporaso et al., 2012). DNA was quantified with a Qubit 3.0 fluorimeter (Life Technologies, Carlsbad, CA) according to manufacturer's instructions following DNA extraction and PCR steps. All samples yielded PCR amplicons when viewed on a gel after initial pre-barcoding PCR (30 cycles). Duplicate PCR reactions were pooled and reconditioned for five cycles with barcoded primers. Samples for sequencing were submitted to Laragen (Culver City, CA) for analysis on an Illumnia MiSeq platform. Sequence data were processed using QIIME version 1.8.0 (Caporaso et al., 2010). Raw sequence pairs were joined and quality-trimmed using the default parameters in QIIME. Sequences were clustered into de novo operational taxonomic units (OTUs) with 99% similarity using UCLUST open reference clustering protocol (Edgar, 2010). Then, the most abundant sequence was chosen as representative for each de novo OTU (Wang et al., 2007). Taxonomic identification for each representative sequence was assigned using the Silva-115 database (Quast et al., 2013) clustered at separately at 99% and at 97% similarity. Singletons and contaminants (OTUs appearing in the negative control datasets) were removed. 16S sequences were aligned using MAFFT (Katoh et al.

2002) and a phylogeny constructed using FastTree (Price et al. 2010). Alpha diversity was estimated using the Shannon Index (Shannon 1948) and Inverse Simpson metric (1/D) (Simpson 1949; Hill 1973) (Table 2). We used the UniFrac distance metric (Lozupone and Knight 2005) to assess the microbial community phylogenetic similarity of microbial communities (Table 3). All statistics were calculated using scripts in QIIME and are reported at the 99% and 97% OTU similarity levels. Multidimensional scaling (MDS) analyses and plots to evaluate the similarity between different samples and OHK environments were produced in R using the vegan and ggplot2 packages (R Core Team 2014, Oksanen et al. 2016, Wickham 2009) (Figure 5).

Metagenomes were sequenced from Pool 1 Sample A (JP1) and Pool 3 Sample A (JP3). DNA was quantified with a Qubit 3.0 fluorimeter (Life Technologies, Carlsbad, CA) according to manufacturer's instructions following DNA extraction. Purified DNA was submitted to SeqMatic LLC (Fremont, CA) for library preparation and sequencing via Illumina HiSeq technology; a single lane of 2x100 sequencing was shared between these two samples and two from another project. Raw sequences were assembled with MegaHit v. 1.02 (Li et al. 2016). Coverage was extracted using bbmap (Bushnell 2016) and samtools (Li et al. 2009). Genes of interest (e.g. coding for ribosomal, photosynthesis, iron oxidation, and electron transport proteins) were identified from assembled metagenomic data locally with BLAST+ (Camacho et al. 2008), aligned with MUSCLE (Edgar 2004), and alignments manually curated in Jalview (Waterhouse et al. 2009). Phylogenetic trees were calculated using RAxML (Stamakis 2014) on the Cipres science gateway (Miller et al. 2010).

Results

Geochemistry

The gas bubbling at the source was determined to contain CO_2, CH_4, and H_2. Source waters were slightly enriched in chloride relative to seawater (~23.2 g/L) but depleted in sulfate (~1.63 g/L) but approached seawater concentrations downstream as mixing increased.

Geochemistry measurements of Jinata source water are summarized in Table 1, while geochemical gradients along the stream outflow are summarized in Table 2. Water emerging from the source was 62°C, very low in dissolved oxygen (~0.15 mg/l), had a pH 5.4, and contained substantial concentrations of dissolved iron (~250 μM Fe^{2+}). After emerging from the source pool, the spring water exchanges gases with the air due to mixing associated with water flow and gas ebullition, and DO rose to 1.24 mg/L at the surface of the source pool. As water flows downstream from the source pool, it cools slightly, exchanges gases with the atmosphere, and intermittently mixes with seawater below Pool 1.

Sequencing

In total, we recovered 456,737sequences from the 10 samples at Jinata (Table 3). Reads per sample ranged from 26,057 Source Pool Sample A to 97,445 for Pool 1 Sample A (median 43,331, mean 45,673, and standard deviation 19,568). Assessment of sampling depth was estimated using Good's Coverage (Good 1953). On average, 74% of the microbial community was recovered from Jinata samples at the 99% OTU level based on

the Good's Coverage statistic (ranging from 54% coverage in the Outflow Sample A to 85% in the Pool 1 Sample A) and 87% at the 97% OTU level (74% for the Outflow Sample A to 94.5% for the Pool 1 Sample B).

Samples from the same site are highly similar, and adjacent sites (e.g. Source and Pool 1, Outflow and Pool 3) show significant similarity. However, there is essentially no overlap in diversity between distant samples (e.g. Source and Outflow).

The assembled contigs from JP1 totaled 334 MB in 331011 contigs. The Pool 3 assembly was 136 MB in 126181 contigs. In order to normalize relative abundance of genes in these two datasets despite their very different sizes, abundance of functional genes were normalized to the number of rpoB genes recovered in each metagenome (sum of distinct sequences assembled multiplied by their coverage). Like the 16S gene, RpoB is a highly conserved, vertically-inherited gene useful for taxonomic identification of organisms, but has the added advantage that it is only known to occur as a single copy per genome (Case et al. 2007). Approximately 11.5x more RpoB genes were recovered in the Pool 1 metagenome than that from Pool 3.

Discussion

Relative abundances of microbial taxa as revealed by 16S surveys can be useful for predicting metabolisms driving geochemical cycles at Jinata (Table 4). In particular, the contributions of various hydrogen- and iron-oxidizers and phototrophs to primary productivity along the spring path can be estimated due to these metabolisms being fairly well conserved within bacterial taxa (e.g. Emerson et al. 2010, Chan et al. 2016). Analysis

of the most abundant taxa at Jinata revealed significant roles for organisms driving aerobic iron and hydrogen oxidation upstream, while Cyanobacteria dominate downstream.

Despite sequencing to relatively high depth (>18000 reads per sample), rarefaction analysis shows that there is still substantial unsequenced diversity at Jinata (Supplemental Figure 1). This likely reflects rather uneven diversity, as >50% of reads at most sites are made up of the 10 most abundant taxa (Table 4). Additional sequencing is therefore likely to reveal additional diversity of rare taxa.

Because only two samples from Jinata were sequenced for shotgun metagenomics, these data cannot be used to interpret the fine scale gradient shown by 16S amplicon sequencing; however, metagenomic results can be used to interpret broad trends between the iron- and hydrogen-dominated upstream sections of the hot spring and the more oxic, lower-iron sections downstream. In particular, the relative abundance of functional metabolic genes associated with processes such as iron oxidation can be compared between these two sites to reinforce interpretations from the 16S data of the metabolic potential of communities in these sites.

Iron and hydrogen oxidation

The hot spring water emerging at the Source Pool at Jinata contains abundant dissolved Fe^{2+} and is continuously bubbling with H_2, and these highly favorable electron donors appear to fuel productivity and determine the microbial community upstream, particularly in the Source Pool and Pool 1 where microbial mats are not well developed.

The most abundant organisms in the Source Pool are members of the Aquificae family Hydrogenothermaceae. This family of marine thermophilic lithotrophs is capable of

both iron and hydrogen oxidation (Takai and Nakagawa 2014), and may be utilizing either or both of these electron donors at Jinata. The seventh most abundant OTU in the Source Pool samples is a novel sequence 89% similar to a strain of *Persephonella*, with relatives found in an alkaline hot spring in Papua New Guinea. *Persephonella* is a genus of thermophilic, microaerophilic hydrogen oxidizing bacteria within the Hydrogenothermaceae (Götz et al. 2002).

The other most abundant organisms near the source are Zetaproteobacteria, related to the neutrophilic, aerobic iron-oxidizing *Mariprofundus* common in marine systems (Emerson et al. 2007). Zetaproteobacteria and Hydrogenothermaceae together made up ~30-65% of sequences in the Source Pool and Pool 1, and so appear to be both numerically dominant as well driving the base of productivity in these environments.

The abundance of Hydrogenothermaceae drops off significantly to less than 1% of sequences downstream of Pool 1 once microbial mats become well developed, but Zetaproteobacteria continue to make up a few percent of reads until the Out Flow. This suggests that shifts in Zetaproteobacteria relative abundance may be due more to the increase in abundance of other organisms, rather than a drop in the number of Zetaproteobacteria or their ability to make a living oxidizing iron. This is consistent with the significant abundance and continual decline in iron concentrations along the flow path of the hot spring.

Members of the Mariprofundaceae have been observed to have an upper growth temperature of 30°C (Emerson et al. 2010). Jinata, with abundant Zetaproteobacteria found at temperatures up to 63 degrees, may represent a unique high-temperature environment for

these organisms. In particular, the third most abundant OTU in the Source Pool and Pool 1 sample A is an unknown sequence which is 92% identical to an uncultured Zetaproteobacteria sequence from a shallow hydrothermal vent in Papua New Guinea (Meyer-Dombard et al. 2013). This sequence likely represents a novel strain of high-temperature iron-oxidizing Zetaproteobacteria.

Members of several phototrophic Proteobacteria lineages were found at Jinata, though not at high relative abundances (<2% of sequences each). These include the Gammaproteobacteria family Chromatiales as well as the Alphaproteobacteria families Rhodospirillales and Rhodobacteraceae. Members of these clades are capable of photoautotrophy using diverse electron donors, including sulfur compounds, H_2 and Fe^{2+} (Imhoff 2014, Pujalte et al. 2014, Baldani et al. 2014), and so it is unclear which if any electron donor is fueling productivity by these organisms at Jinata.

The diversity of iron oxidizing bacteria at Jinata is very different than in other iron-rich hot springs. For example, at Oku-Okuhachikurou Onsen in Akita Prefecture, Japan, iron oxidation is driven primarily by the Gammaproteobacteria *Gallionella (*Ward et al. 2017), while at Chocolate Pots hot spring at Yellowstone National Park iron oxidation is driven primarily by oxygen produced *in situ* by Cyanobacteria (Pierson et al 1999). This may be related to selection by the highly saline water, or biogeographically by access to the ocean, as Zetaproteobacteria are typically found in marine settings, particularly in deep ocean basins associated with hydrothermal iron sources (Emerson et al. 2010). Similarly to Oku-Okuhachikurour Onsen, Jinata supports only limited biomass in regions dominated by iron oxidizers (Ward et al. 2017), reflecting the shared biochemistry and bioenergetic

challenges of neutrophilic iron oxidation by *Gallionella* and Zetaproteobacteria (Kato et al. 2015, Bird et al. 2011).

The relative abundance of genes associated with iron oxidation in the Pool 1 and Pool 3 metagenomes reflect the organismal abundance revealed by 16S amplicon sequencing. Diversity and coverage of foxE, mobB, and pioA—associated with iron oxidation in *Rhodobacter*, *Mariprofundus*, and *Rhodopseudomonasi*, respectively—were present at much higher abundance in the Pool 1 metagenome than Pool 3 (mobB and pioA at 4-5x higher relative abundance in Pool 1, while foxE was of similar abundance in Pool 1 to pioA but absent from the Pool 3 metagenome).

Cyanobacteria

Cyanobacteria are nearly absent from near the source pool, but begin to appear around Pool 1 and become dominant starting in Pool 2. The most abundant Cyanobacteria present are predominantly members of Subsection III, Family I. This group includes *Leptolyngbya*, a genus of filamentous non–heterocystous Cyanobacteria that has appeared in other hot springs of similar temperatures (e.g. Ward et al. 2017, Roeselers et al. 2007, Bosak et al. 2012). Cyanobacteria, performing oxygenic photosynthesis, appear to dominate primary productivity in downstream regions of the hot spring, and the filamentous morphology of the strains present here allow them to contribute to the cohesive fabric of the microbial mat.

In the Out Flow samples, Chloroplast sequences become abundant, most closely related to the diatom *Melosira*. Algae are at very low abundance upstream of the Out Flow,

potentially inhibited by high temperatures, high iron concentrations, or other characteristics of the hot spring water, but the higher seawater influence at the Out Flow creates a more permissive environment.

Cyanobacteria are sometimes underrepresented in iTag datasets as a result of poor DNA yield or amplification biases (e.g. Parada et al. 2015, Trembath-Reichert et al. 2016), but the low abundance of Cyanobacteria near the Source Pool was confirmed by fluorescent microscopy, in which cells displaying cyanobacterial autofluorescence were observed abundantly in samples from the downstream samples but not in the Source Pool (Figure 4).

Methane cycling

Methane is present in the bubbles emerging from the Source Pool at Jinata. No sequences associated with known methanogens were recovered from Jinata, suggesting that the methane found here may have an abiotic thermal source. This presence of methane does however provide a niche for methane oxidizing microbes, particularly aerobic methanotrophic bacteria. An abundant 16S sequence in the Source Pool and Pool 1 is most similar (94%) to that from *Methylomarinovum caldicuralii*, a thermophilic aerobic methanotroph from a hydrothermal vent in Japan (Hirayama et al. 2014), and so may represent a related strain involved in methane oxidation at Jinata. Related species in the *Methylothermaceae* family have recently been shown to also be capable of denitrification,

potentially coupled to methane oxidation (Skennerton et al. 2015) raising the possibility that members of this clade are more metabolically versatile than expected.

Anaerobic respiration

The amount of sulfur cycling occurring at Jinata likely varies significantly along stream. This is reflected in the relative abundance of common sulfate reducing bacteria such as the Deltaproteobacterium *Desulforomonas*, which increases greatly downstream. Sulfate is abundant throughout Jinata, but more thermodynamically favorable electron donors like oxygen and iron oxide likely make sulfate reduction unfavorable except within dense microbial mats. Furthermore, the presence of high concentrations of dissolved iron upstream make sulfide unstable, as it will rapidly precipitate as iron sulfide minerals like pyrite, reducing the ability of the microbial community to cycle sulfur effectively— conditions analogous to those in the dominantly ferruginous Archean ocean (Walker and Brimblecombe 1985).

The Deferribacteres phylum is present at up to ~2% relative abundance in some samples. The Deferribacteres is made up of thermophiles with diverse anaerobic respiratory pathways, including the reduction of iron, nitrate, or manganese (Garrity et al. 2001). Given the abundance of poorly ordered iron oxides like ferrihydrite at Jinata, iron reduction is a favorable anaerobic respiration pathway, creating a likely niche for these organisms.

Nitrogen cycling

Ammonia is fairly abundant in the source water of Jinata (~1.56 mg/L), and is still detectable by the outflow (~0.56 mg/L), suggesting that nitrogen is not a limiting nutrient in this hot spring. Some biological nitrogen cycling may be occurring, as evidenced by the

presence of sequences associated with nitrifying microbes. This includes Marine Group 1 Thaumarchaeota (up to 3% abundance in Pool 2), a clade made up of ammonia oxidizing archaea such as *Nitrosopumilus maritimus* (Pester et al. 2011). The family Nitrospiraceae in the Nitrospira phylum was present at up to ~2% abundance in upstream samples at Jinata. The Nitrospiraceae include the nitrite oxidizing *Nitrospira*, but the family is metabolically diverse and also includes aerobic iron oxidizers and both heterotrophic and hydrogenotrophic sulfate reducers (Daims 2014). However, the three most abundant OTUs affiliated with the Nitrospiraceae at Jinata are most similar to *Thermodesulfovibrio*, thermophilic, hydrogenotrophic or heterotrophic sulfate reducing bacteria (Daims 2014). A smaller number of 16S reads were associated with the *Nitrospira*, primarily recovered from Pool 1 Sample A; this is consistent with substantial coverage of nitrite oxidoreductase genes recovered from the metagenome collected from this site. The spike in relative abundance of *Nitrospira* where Pool 1 flows into Pool 2 may be a result of cooling of the hot spring water across the upper temperature limit of these organisms, as the upper temperature limit for cultured members of this genus is 52°C (Lebedeva et al. 2011).

Other organisms

Members of Subgroup 22 of the Acidobacteria phylum were abundant at Jinata. The Acidobacteria phylum is subdivided into 26 subgroups (Barns et al. 2007), yet only six contain well-characterized members (Kielak et al. 2016). This does not include Subgroup 22, and so it is unknown what role Acidobacteria may play at Jinata, but the abundance of these organisms at Jinata may make this hot spring a valuable resource for their characterization.

Members of the Chloroflexi class Anaerolineae are common throughout Jinata with the exception of the Outflow. The Anaerolineae have generally been isolated as obligately anaerobic heterotrophs (e.g. Sekiguchi et al. 2003, Yamada et al. 2006), but genome sequencing has revealed the capacity for aerobic respiration in diverse members of this clade (e.g. Hemp et al. 2015ab, Pace et al. 2015, Ward et al. 2015a). Furthermore, phototrophy has been described in a close relative of this class from a Yellowstone National Park metagenome (Klatt et al. 2011), further hindering attempts to interpret the metabolism and ecology of members of this genome from 16S data alone.

Additionally, members of the Chloroflexi class Caldilineae were present at up to ~1% abundance at Jinata. Members of the Caldilineae have previously been isolated form intertidal hot springs in Iceland (Kale et al. 2013) and Japanese hot springs (Sekiguchi et al. 2003) and placed into a separate class in the Chloroflexi sister to the Anaerolineae (Yamada et al. 2006). Characterized organisms in this class are filamentous, anaerobic, or facultatively aerobic heterotrophs and therefore may play a role in degrading biomass within low-oxygen regions of microbial mats.

Members of the Bacteroidetes phylum are abundant at Jinata, particularly in Pool 2 and Pool 3 where cyanobacterial mats are well developed. The Bacteroidetes sequences found are primarily members of the Sphingobacterales families Saprospiraceae and Chitinophagaceae. Saprospiraceae are commonly involved in the breakdown of complex organic matter in marine environments (McIllroy and Nielsen 2014), while members of the Chitinophagaceae are known to degrade biopolymers like cellulose and chitin (Rosenberg 2014), suggesting a possible role for these organisms in the degradation of extracellular

polymeric substances in the microbial mats at Jinata. The Verrucomicrobia family Opitutaceae is also abundant in microbial mats at Jinata, and is typically associated with the degradation of recalcitrant heteroppolysaccharides in a variety of contexts including marine and hot spring environments (Rodrigues and Isanapong 2014) and may fill a similar niche.

The Planctomycete family Phycisphaeraceae was also at relatively high abundance in Pool 2 and Pool 3. This lineage was first isolated from marine algae on Mikura-jima, part of the Izu Islands of which Shikinejima is a part (Fukunaga et al. 2009). Additional strains of Phycisphaeraceae have since been isolated in association with marine algae (Yoon et al. 2014), suggesting that Phycisphaeraceae at Jinata may also occur in association with algae at Jinata.

Members of the WS3 phylum, also known as Latescibacteria, are closely related to the Bacteroidetes as part of the CFB superphylum, and have been described as anaerobic fermenters that break down algal polysaccharides (Youssef et al. 2015). Members of the WS3 phylum may play a similar role at Jinata, but are most abundant in Pool 1, where microbial mats are absent and algae are at very low abundance, so it is possible that they fill a different niche.

Conclusions

Jinata Onsen is a novel environment supporting strong geochemical gradients over short spatial scales. The transition from low-oxygen, iron- and hydrogen-rich hot spring source water to oxygen-rich ocean water takes place over just a few meters, and results in an almost complete change in microbial community. This system is significant for its

relevance as a process analog for environments through Earth history and potentially habitable environments in Mars' past, and for its utility as environment to investigate iron-tolerant Cyanobacteria.

Over the course of ~1.5 billion years in the Proterozoic eon, the ocean underwent major geochemical and redox shifts from anoxic, iron-rich Archean oceans to its modern oxygen- and sulfate-rich state (Lyons et al. 2014). This major change in ocean geochemistry was reciprocally impacted by changes in the organisms and metabolisms used to drive primary production and other geochemical cycles. Through the Archean eon, the ocean was anoxic and iron-rich, and productivity is thought to have been driven primarily by iron- and hydrogen-oxidizing microbes (Kharecha et al. 2005, Canfield et al. 2006). At this time, and during the beginning of the Proterozoic, oxygenic Cyanobacteria were absent or unproductive (Fischer et al. 2016). Following the Great Oxygenation event ~2.3 billion years ago, oxygen accumulated to low but non-negligible levels in the atmosphere, and the surface ocean became oxygenated though the deep ocean remained anoxic and was variably rich in either free sulfide or ferrous iron (Poulton et al. 2010). Cyanobacteria and aerobic metabolisms became more significant, but anaerobic and anoxygenic organisms continued to contribute to productivity (Brocks et al. 2005, Johnston et al. 2009). Finally, during the Neoproterozoic, atmospheric oxygen reached modern levels and the deep ocean became well oxygenated (Saito et al. 2012). Since this time, marine productivity has been dominated by Cyanobacteria and eukaryotic algae (Geider et al. 2001).

These shifts in open ocean conditions took place over ~1.5 billion years, yet a full range of analogous conditions are recapitulated in some ways over a spatial scale of just a few meters at Jinata. The Source Pool, with its low oxygen, abundant ferrous iron and molecular hydrogen, and productivity dominated by lithotrophs and anoxygenic phototrophs in the absence of Cyanobacteria, is comparable to conditions in the earliest Paleoproterozoic, leading up to the Great Oxygenation Event. The gradual increase of oxygen and sulfate concentrations and loss of iron and hydrogen going downstream is comparable to middle Proterozoic time, when Cyanobacteria and anoxygenic phototrophs coexisted in a redox-stratified ocean. Finally, with a transition to fully oxygenated conditions and modern marine chemistry and the appearance of productive eukaryotic algae, the Out Flow at Jinata is representative of relatively modern ocean conditions that first developed in the Neoproterozoic. While other analog systems exist for each of these time periods (e.g. ferruginous Lake Matano in Indonesia as an Archean analog, Crowe et al. 2008, and Oku-Okuhachikurou Onsen in Japan as a Paleoproterozoic analog, Ward et al. 2017), these systems are incredibly disparate and challenging to compare directly. As a result of Jinata reflecting aspects of such a long span of Earth history over such a short spatial scale, this system allows comparison of very different geochemical contexts while avoiding extraneous confounding variables that plague comparisons of more disparate analog field sites, such as differences in biogeography, nutrient availability, or extreme differences in salinity or pH.

By observing trends in microbial diversity and community function across this gradient in geochemical conditions at Jinata, we can make predictions about how the

biosphere on the early Earth may have functioned. By observing, for instance, the relative productivity and abundance of aerobic iron- and hydrogen-oxidizers relative to anoxygenic phototrophs in the Source Pool we may be able to make predictions about the relative contribution of these metabolisms to the deposition of Banded Iron Formations through Earth history (e.g. Konhauser et al. 2002), while comparison of the net community productivity between the Source Pool and downstream regions we can predict how global productivity may have changed over Proterozoic time as oxygenic phototrophs began to dominate. The proximal cause of the GOE, and the transition toward a more oxygen-rich and iron-poor ocean, is contested; this event may record the late evolution of oxygenic Cyanobacteria (e.g. Ward et al. 2016, Shih et al. 2016, Fischer et al. 2016), or may reflect a delayed expansion of cyanobacterial productivity due to geochemical or geological conditions (e.g. Kasting 2013). Similarly, the Neoproterozoic saw a shift from productivity driven by Cyanobacteria and anoxygenic phototrophs to Cyanobacteria and eukaryotic algae (Johnston et al. 2009). Though again, whether the shift in dominant primary producers at this time was a result of the late evolution of eukaryotic algae (e.g. Shih and Matzke 2013) or due to a shift in geochemical conditions (e.g. Anbar and Knoll 2002) is unclear. Characterization of the factors controlling dominant primary producers along the flow path of Jinata could help build hypotheses for these historical transitions, as Jinata provides a case where the full suite of primary producers area present but a clear succession from hydrogen- and iron-driven metabolisms, to Cyanobacteria, to eukaryotic algae occurs along the flow path of the hot spring. Constraining what factors drive this transition—oxygen or iron concentrations, trace element abundance, or other factors that may or may

not be relevant to the Proterozoic ocean—may help to predict the drivers for historical shifts in productivity as well.

Jinata is also a valuable resource for investigating the ecology and mineralogical records of iron-oxidizing Zetaproteobacteria in an environment which is much more accessible than other Zetaproteobacteria-rich systems such as those at Loihi Seamount (e.g. Chan et al. 2016). Characterization of Zetaproteobacteria *in situ* is particularly valuable for characterizing the production and preservability of mineralogical signatures of these organisms. The iron oxides precipitated as a byproduct of their metabolism can retain distinctive morphologies, including "stalks" produced by Zetaproteobacteria like *Mariprofundus* (Chan et al. 2011). These iron microfossils can be preserved over geological timescales and so are useful for interpreting the role of iron oxidizing bacteria in past environments (Krepski et al. 2013), and may help diagnose what if any role aerobic iron oxidizing bacteria like the Zetaproteobacteria played in the deposition of Proterozoic Banded Iron Formations (Chan et al. 2016b).

Furthermore, our observations at Jinata are relevant for interpretations of the environmental constraints on cyanobacterial productivity in the Archean and early Proterozoic when dissolved ferrous iron is thought to have been abundant in the oceans. Previously, it has been suggested that high ferrous iron concentrations are toxic to Cyanobacteria, greatly reducing their potential for productivity under ferruginous conditions that may have persisted through much of the Archean era (Swanner et al. 2015). The high rates of cyanobacterial productivity observed at Jinata under high iron concentrations suggest that Cyanobacteria can adapt to ferruginous conditions, and

therefore iron toxicity is unlikely to inhibit Cyanobacteria over geological timescales. In fact, the iron concentrations observed at Jinata are much higher (150-250 μM) than predicted for the Archean ocean (<120 μM, Holland 1984) or observed at other iron-rich hot springs (~100-200 μM, Pierson et al. 1999, Ward et al. 2017), making Jinata an excellent test case for determining the ability of Cyanobacteria to adapt to high iron concentrations. Culture-based experiments may be useful to determine whether Jinata Cyanobacteria utilize similar strategies to other iron-tolerant strains (e.g. the *Leptolyngbya*-relative *Marsacia ferruginose*, Brown et al. 2010) or whether Jinata strains possess unique adaptations that allow them to grow at higher iron concentrations than known for other environmental Cyanobacteria strains, as well as whether the paucity of Cyanobacteria in the Source Pool and Pool 1 are due to the >260 μM iron concentrations or a result of other factors like high temperatures.

Finally, the dynamic abundances of redox-active compounds oxygen, iron, hydrogen, and sulfate at Jinata may not only be analogous to conditions on the early Earth, but may have substantial relevance for potentially habitable environments on Mars as well. Early Mars is thought to have supported environments with metabolic opportunities provided by the redox gradient between the oxidizing atmosphere and abundant electron donors such as ferrous iron and molecular hydrogen sourced from water/rock interactions (e.g. Hurowitz et al. 2010). Uncovering the range of microbial metabolisms present under the environmental conditions at Jinata, and their relative contributions to primary productivity, may therefore find application to predicting environments on Mars most able to support productive microbial communities.
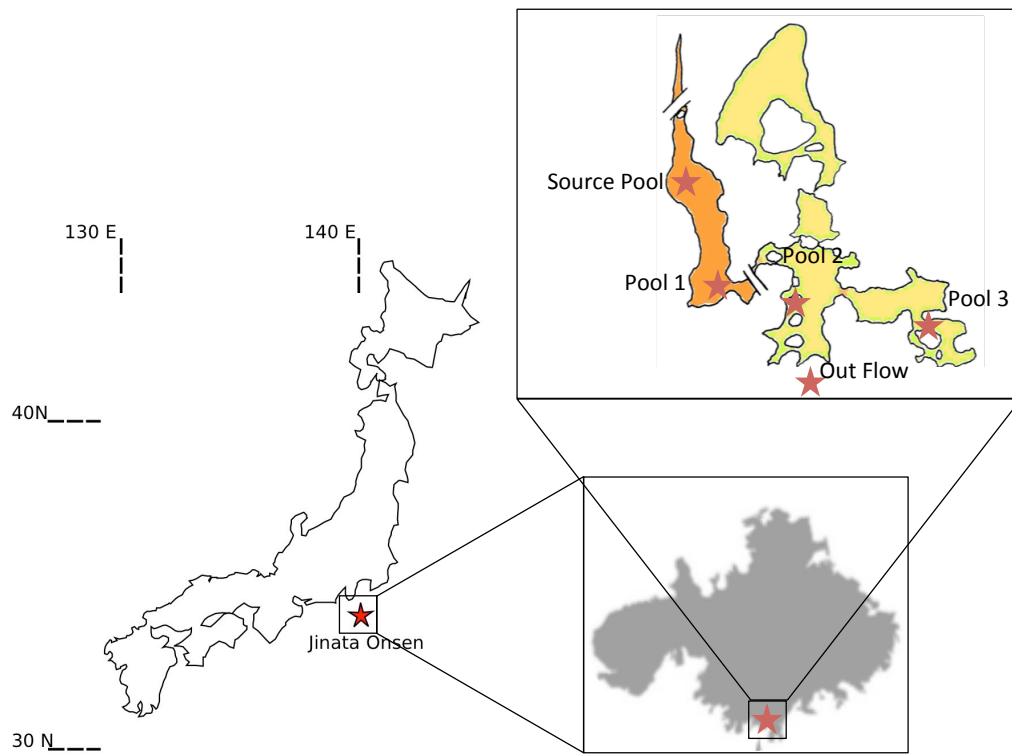
Figure 1:

Location of Jinata Onsen on Shikinejima Island, Japan, and inset overview sketch of field site with sampling localities marked.

Figure 2:

Representative photos of Jinata. A) Panorama of field site, with source pool on left (Pool 1 below), Pool 2 and 3 in center, and Out Flow to bay on right. B) Undistorted view north up the canyon. C) Undistorted view south toward bay, overlooking Pool 2. D) Source pool, coated in floc-y iron oxides and bubbling with gas mixture containing H2, CO2, and CH4. E) Pool 2, with mixture of red iron oxides and green from Cyanobacteria-rich microbial mats. F) Close up of textured microbial mats in Pool 3. G) Close up of Out Flow, where hot spring water mixes with ocean water.

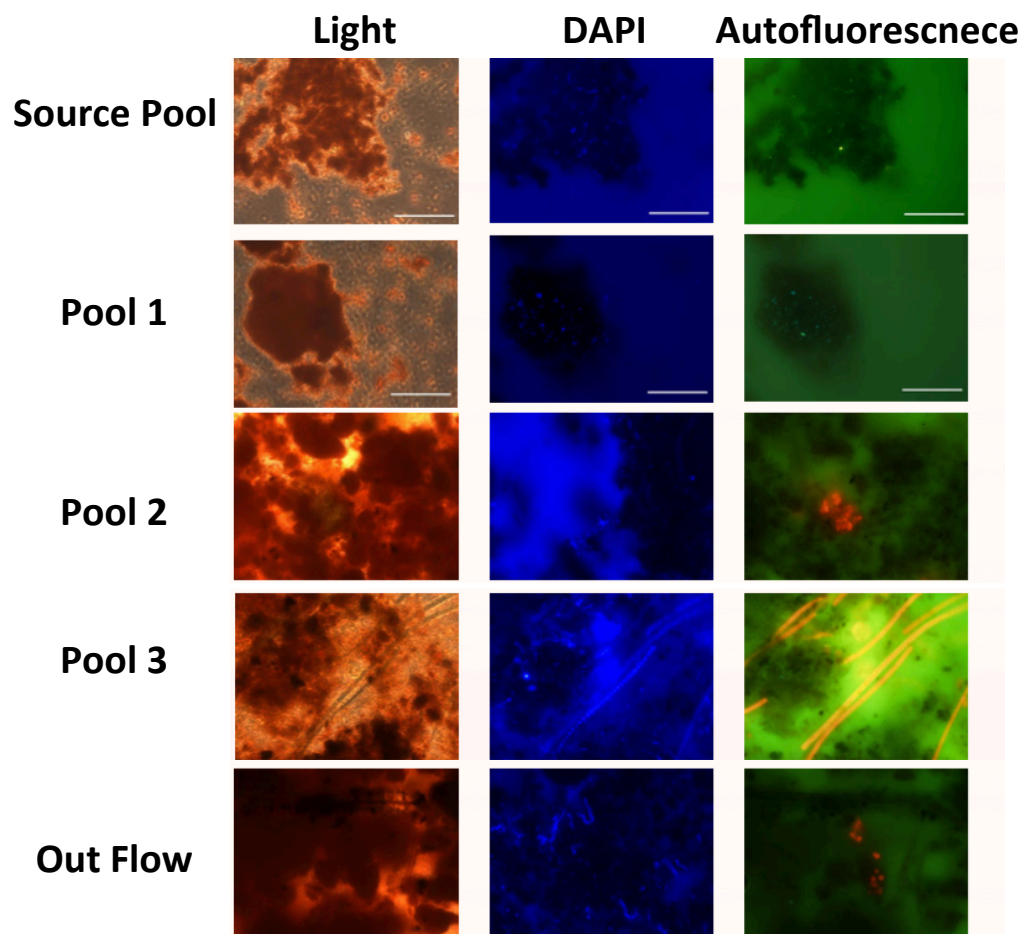|	Light	DAPI	Autofluorescnece
Source Pool			
Pool 1			
Pool 2			
Pool 3			
Out Flow			

Figure 3

Microscopy images of sediment (Source and Pool 1) or mat (Pool 2, Pool 3, and Out Flow). Left are light microscopy images. Center and right are fluorescence images. At center, blue signal is DAPI-stained (Excitation: 365nm, Emission: BP445~50nm). At right, red is autofluorescence signal of Cyanobacteria (BP395~440nm, LP470nm). Scale bars 50 μm.
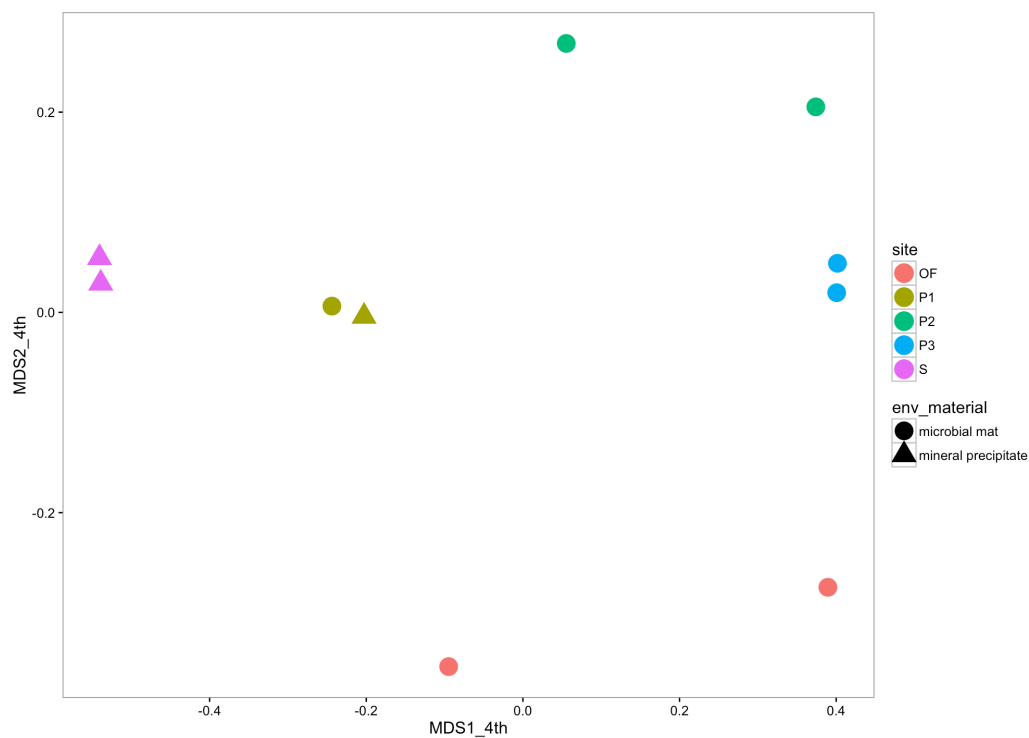
Figure 4:

Multidimensional scaling plot of Jinata samples. Each point represents the recovered microbial community from a given sample, with sites identified by color and sample type by shape. Samples plotting close to each other are relatively more similar in community composition. Abundance data are transformed by the 4th root to down-weight the effect of abundant taxa. Stress value is 0.0658.

T	63°C
pH	5.4
DO	4.7 μM
Fe^{2+}	261 μM
NH$_3$/NH$_4^+$	87 μM
Cl$^-$	654 mM
SO$_4^{--}$	17 mM
NO$_3^-$	b.d.
NO$_2^-$	b.d.
HPO$_4^-$	b.d.

Table 1:

Geochemical characteristics of Jinata source water. Nitrate, nitrite, and phosphate were below the detection limit of ~0.1 mg/L.

	pH	T (°C)	Fe(II) (μM)	DO (μM)	Descriptions
Source	5.4	60-63	260	4.7 (source) 39 (surface)	Fluffy red iron oxide precipitate
Pool 1	5.8	59-59.5	265	58	Reddish precipitate and streamers in shallower regions, more yellowish deeper
Pool 2	6.5	44.5-54	151	134	Iron oxide-coated microbial mats. Orange to orange-green.
Pool 3	6.7	37.3-46	100	175	Green or mottled orange-green microbial mats, commonly with 1-5cm finger-like morphology.
Outflow	6.5	27-32	45	234	Ocean water within mixing zone at high tide, with constant flow of spring water from Pool 2. Thin green microbial mats.

Table 2:
Summary table, showing overall geochemical transition from iron-rich hot spring source to

dominantly marine outflow.

| Sample:	Reads:	OTUs (99%)	Good Coverage (99%):	Shannon Index (99%):	Inverse Simpson (99%):	OTUs (97%)	Goods Coverage (97%)	Shannon Index (97%)	Inverse Simpson (97%):
Source bottom	26057	9558	0.724	10.594	83.020	4632	0.884	8.196	23.035
Source top	49340	14392	0.790	10.275	44.714	5530	0.932	7.229	12.835
Pool 1 A	97445	21166	0.848	10.128	56.287	10160	0.935	8.080	24.682
Pool 1 B	57250	10559	0.872	8.794	33.323	4766	0.945	6.414	12.005
Pool 2 A	41515	13114	0.759	9.754	24.340	7710	0.873	8.118	14.702
Pool 2 B	45171	17211	0.697	10.708	50.836	10525	0.832	8.980	25.783
Pool 3 A	45148	15988	0.722	10.287	33.295	9302	0.853	8.351	16.880
Pool 3 B	29778	12023	0.682	10.894	84.725	6625	0.837	8.553	31.520
Outflow A	32382	17741	0.542	11.931	57.572	11290	0.738	10.262	28.674
Outflow B	32651	8881	0.797	9.237	28.728	4210	0.909	6.373	9.850

Table 3:

Diversity metrics of Jinata sequencing. Diversity metrics calculated for both 99% and 97%

sequence identity cutoffs for assigning OTUs.

Taxon	S.A	S.B	P1.A	P1.B	P2.A	P2.B	P3.A	P3.B	OF.A	OF.B	
Bacteria;__Cyanobacteria;__Cyanobacteria;__SubsectionIII;__FamilyI	0.06%	0.02%	2.20%	0.48%	0.32%	17.63%	29.96%	23.25%	22.36%	37.44%	13.37%
Bacteria;__Proteobacteria;__Zetaproteobacteria;__Mariprofundales;__Mariprofundaceae	14.07%	29.96%	24.89%	29.72%	4.26%	1.89%	1.52%	0.78%	3.28%	0.54%	11.09%
Bacteria;__Aquificae;__Aquificae;__Aquificales;__Hydrogenothermaceae	30.54%	34.24%	3.54%	25.38%	0.21%	0.08%	0.16%	0.20%	0.55%	0.59%	9.55%
Bacteria;__Cyanobacteria;__Chloroplast;__o;__f	0.10%	0.01%	1.39%	0.15%	0.20%	0.14%	0.22%	0.40%	0.56%	33.11%	3.63%
Bacteria;__Chloroflexi;__Anaerolineae;__Anaerolineales;__Anaerolineaceae	5.66%	1.68%	4.45%	1.69%	3.23%	9.49%	2.87%	5.41%	0.30%	0.28%	3.50%
Bacteria;__Bacteroidetes;__Sphingobacteriia;__Sphingobacteriales;__Chitinophagaceae	0.05%	0.04%	0.08%	0.09%	0.15%	5.71%	10.93%	9.32%	1.18%	0.15%	2.77%
Bacteria;__Cyanobacteria;__Cyanobacteria;__SubsectionII;Other	0.00%	0.00%	0.07%	0.08%	24.47%	0.07%	0.19%	0.32%	0.10%	0.41%	2.57%
Bacteria;__Bacteroidetes;__Sphingobacteriia;__Sphingobacteriales;__Saprospiraceae	0.01%	0.02%	0.40%	0.12%	5.70%	6.53%	1.84%	0.36%	4.36%	3.02%	2.23%
Bacteria;__Planctomycetes;__Phycisphaerae;__Phycisphaerales;__Phycisphaeraceae	0.00%	0.00%	4.47%	0.08%	3.22%	2.75%	3.32%	6.68%	1.14%	0.15%	2.18%
Bacteria;__Cyanobacteria;__Cyanobacteria;Other;Other	0.01%	0.01%	0.18%	0.13%	0.21%	0.44%	3.21%	10.82%	0.71%	3.71%	1.94%
Bacteria;__Proteobacteria;Other;Other;Other	1.17%	1.92%	2.25%	10.48%	0.58%	0.50%	0.25%	0.22%	0.87%	0.08%	1.83%
Bacteria;__Acidobacteria;__Subgroup_22;__o;__f	0.53%	0.34%	5.21%	1.39%	8.16%	0.21%	0.36%	0.32%	0.18%	0.12%	1.68%
Bacteria;__Verrucomicrobia;__Opitutae;__Opitutales;__Opitutaceae	0.00%	0.00%	0.02%	0.03%	0.05%	2.23%	6.64%	1.16%	2.05%	0.05%	1.22%
Bacteria;__Proteobacteria;__Alphaproteobacteria;__Rhodobacterales;__Rhodobacteraceae	0.34%	0.26%	0.72%	0.31%	1.98%	2.00%	2.05%	0.92%	1.79%	1.19%	1.15%
Bacteria;__Proteobacteria;__Deltaproteobacteria;__Desulfuromonadales;Other	0.02%	0.02%	0.11%	0.16%	0.03%	0.68%	0.43%	0.21%	9.76%	0.07%	1.15%
Bacteria;__Proteobacteria;__Gammaproteobacteria;Other;Other	2.64%	1.74%	2.26%	1.99%	0.31%	0.55%	0.25%	0.26%	0.60%	0.25%	1.08%
Bacteria;__Deferribacteres;__Deferribacteres;__Deferribacterales;__Family_Incertae_Sedis	0.85%	0.20%	2.07%	0.40%	1.94%	0.32%	1.43%	0.57%	0.16%	0.09%	0.80%
Bacteria;__Planctomycetes;__Planctomycetacia;__Planctomycetales;__Planctomycetaceae	0.26%	0.06%	1.08%	0.60%	3.37%	1.06%	0.32%	0.17%	0.22%	0.17%	0.73%
Bacteria;__Chloroflexi;__Caldilineae;__Caldilineales;__Caldilineaceae	0.16%	0.06%	1.07%	0.20%	0.99%	0.64%	1.35%	0.44%	0.21%	0.02%	0.51%
Bacteria;__Nitrospirae;__Nitrospira;__Nitrospirales;__Nitrospiraceae	2.18%	0.30%	0.66%	0.26%	1.15%	0.10%	0.03%	0.05%	0.03%	0.07%	0.48%
Bacteria;__Proteobacteria;__Alphaproteobacteria;__Rhodospirillales;__Rhodospirillaceae	0.05%	0.05%	1.02%	0.81%	0.78%	0.71%	0.32%	0.11%	0.70%	0.09%	0.46%
Archaea;__Thaumarchaeota;__Marine_Group_I;Other;Other	0.00%	0.00%	0.01%	0.00%	3.09%	0.19%	0.01%	0.03%	0.02%	0.02%	0.34%
Bacteria;__Candidate_division_WS3;__c;__o;__f	0.15%	0.03%	1.21%	0.23%	0.15%	0.08%	0.07%	0.03%	0.12%	0.09%	0.22%
Bacteria;__Proteobacteria;__Gammaproteobacteria;__Chromatiales;__Chromatiaceae	0.23%	0.24%	0.21%	0.08%	0.23%	0.02%	0.03%	0.02%	0.03%	0.00%	0.11%
Bacteria;__Proteobacteria;__Alphaproteobacteria;__Rhodospirillales;Other	0.06%	0.01%	0.13%	0.09%	0.42%	0.10%	0.05%	0.03%	0.03%	0.00%	0.09%

Table 4:

Relative abundance of taxa to the Family level. Overall 10 most abundant taxa listed, as well as other taxa of interest mentioned in the text.

Supplemental Information:

observed_species: SampleID
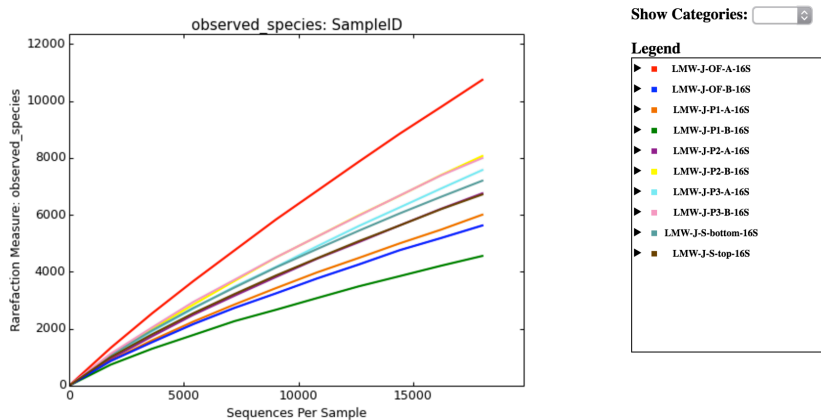
Supplemental Figure 1:

Rarefaction curves of Jinata samples. Sampling depth is down sampled to 18000 reads for sample.

	S-top	OF-B	OF-A	S-bottom	P2-A	P2-B	P1-A	P3-A	P3-B	P1-B
S-top	0.000	0.934	0.772	0.219	0.809	0.843	0.553	0.829	0.870	0.268
OF-B		0.000	0.651	0.964	0.863	0.808	0.844	0.669	0.665	0.911
OF-A			0.000	0.783	0.797	0.500	0.662	0.461	0.551	0.734
S-bottom				0.000	0.797	0.830	0.550	0.829	0.866	0.320
P2-A					0.000	0.755	0.612	0.803	0.820	0.744
P2-B						0.000	0.692	0.442	0.480	0.790
P1-A							0.000	0.696	0.735	0.426
P3-A								0.000	0.268	0.795
P3-B									0.000	0.840
P1-B										0.000

Supplemental Table 1:

Weighted Unifrac matrix, showing the dissimilarity between samples, incorporating both differences in presence/absence as well as relative abundance of taxa (color coded to highlight relative dissimilarity—dark green is <0.33 dissimilarity, pale green >0.33 and <0.5, yellow >0.5 and <0.66, orange >0.66).

References

1. Anbar, a D. & Knoll, a H. Proterozoic ocean chemistry and evolution: a bioinorganic bridge? *Science* **297,** 1137–1142 (2002).

2. Baldani, José Ivo, et al. "The family rhodospirillaceae." *The Prokaryotes*. Springer Berlin Heidelberg, 2014. 533-618.

3. Barns, Susan M., Shannon L. Takala, and Cheryl R. Kuske. "Wide distribution and diversity of members of the bacterial kingdom Acidobacterium in the environment." *Applied and environmental microbiology* 65.4 (1999): 1731-1737.

4. Bird, L. J., Bonnefoy, V. & Newman, D. K. Bioenergetic challenges of microbial iron metabolisms. Trends Microbiol. 19, 330–340 (2011).

5. Bosak, T. et al. Cyanobacterial diversity and activity in modern conical microbialites. Geobiology 10, 384–401 (2012).

6. Brocks, J. J. et al. Biomarker evidence for green and purple sulphur bacteria in a stratified Palaeoproterozoic sea. Nature 437, 866–870 (2005).

7. Brown, Igor I., et al. "Polyphasic characterization of a thermotolerant siderophilic filamentous cyanobacterium that produces intracellular iron deposits." *Applied and environmental microbiology* 76.19 (2010): 6664-6672.

8. Bushnell, B. "BBMap short read aligner." *University of California, Berkeley, California. URL http://sourceforge.net/projects/bbmap* (2016).

9. Camacho C., Coulouris G., Avagyan V., Ma N., Papadopoulos J., Bealer K., & Madden T.L. (2008) "BLAST+: architecture and applications." BMC Bioinformatics 10:421.

10. Canfield, D. E., Rosing, M. T. & Bjerrum, C. Early anaerobic metabolisms. *Philos. Trans. R. Soc. B Biol. Sci.* **361,** 1819–1836 (2006).

11. Caporaso, J. G. et al. Ultra-high-throughput microbial community analysis on the Illumina HiSeq and MiSeq platforms. ISME J 6, 1621–1624 (2012).

12. Caporaso, J. Gregory, et al. "QIIME allows analysis of high-throughput community sequencing data." Nature methods 7.5 (2010): 335-336.

13. Case, R. J. *et al.* Use of 16S rRNA and rpoB genes as molecular markers for microbial ecology studies. *Appl. Environ. Microbiol.* **73,** 278–288 (2007).

14. Catling, D. C., Glein, C. R., Zahnle, K. J. & McKay, C. P. Why O2 is required by complex life on habitable planets and the concept of planetary 'oxygenation time'. *Astrobiology* **8,** 377–395 (2005).

15. Chan, Clara S., et al. "Lithotrophic iron-oxidizing bacteria produce organic stalks to control mineral growth: implications for biosignature formation." *The ISME journal* 5.4 (2011): 717-727.

16. Chan, Clara S., et al. "The architecture of iron microbial mats reflects the adaptation of chemolithotrophic iron oxidation in freshwater and marine environments." *Frontiers in Microbiology* 7 (2016).

17. Chan, C. S., Emerson, D. & Luther, G. W. The role of microaerophilic Fe-oxidizing micro-organisms in producing banded iron formations. *Geobiology* **14,** 509–528 (2016b).

18. Crowe, S. A. et al. Photoferrotrophs thrive in an Archean Ocean analogue. Proc. Natl. Acad. Sci. 105, 15938–15943 (2008).

19. Daims, Holger. "The family nitrospiraceae." *The Prokaryotes*. Springer Berlin Heidelberg, 2014. 733-749.

20. Edgar RC. 2010. Search and clustering orders of magnitude faster than BLAST. Bioinformatics 26(19):2460-2461.

21. Ehrenreich, A., and Widdel, F., 1994, Anaerobic oxidation of ferrous iron by purple bacteria, a new type of phototrophic metabolism: Applied and Environmental Microbiology, v. 60, p. 4517–4526

22. Emerson, D. *et al*. A novel lineage of proteobacteria involved in formation of marine Fe-oxidizing microbial mat communities. *PLoS One* **2,** (2007).

23. Emerson, D., Fleming, E. J. & McBeth, J. M. Iron-oxidizing bacteria: an environmental and genomic perspective. Annu. Rev. Microbiol. 64, 561–583 (2010).

24. Fischer, W., Hemp, J. & Johnson, J. E. Evolution of Oxygenic Photosynthesis. Annu. Rev. Earth Planet. Sci. 44, (2016).

25. Fukunaga, Y. *et al*. Phycisphaera mikurensis gen. nov., sp nov., isolated from a marine alga, and proposal of Phycisphaeraceae fam. nov., Phycisphaerales ord. nov and Phycisphaerae classis nov in the phylum Planctomycetes. *J. Gen. Appl. Microbiol*. **55,** 267–275 (2009).

26. Garrity, George M., et al. "Phylum BIX. Deferribacteres phy. nov." *Bergey's Manual® of Systematic Bacteriology*. Springer New York, 2001. 465-471.

27. Geider, Richard J., et al. "Primary productivity of planet earth: biological determinants and physical constraints in terrestrial and aquatic habitats." *Global Change Biology* 7.8 (2001): 849-882.

28. GOOD, I.J., 1953, The population frequencies of species and the estimation of population parameters: Biometrika, v. 40, p. 237–264.

29. Götz, D., et al. "Persephonella marina gen. nov., sp. nov. and Persephonella guaymasensis sp. nov., two novel, thermophilic, hydrogen-oxidizing microaerophiles from deep-sea hydrothermal vents." International Journal of Systematic and Evolutionary Microbiology 52.4 (2002): 1349-1359.

30. Hemp J, Ward LM, Pace LA, Fischer WW. 2015. Draft genome sequence of Levilinea saccharolytica KIBI-1, a member of the Chloroflexi class Anaerolineae. Genome Announc 3(6):e01357-15.

31. Hemp J, Ward LM, Pace LA, Fischer WW. 2015. Draft genome sequence of Ornatilinea apprima P3M-1, an anaerobic member of the Chloroflexi class Anaerolineae. Genome Announc 3(6):e01353-15.

32. Hemp J, Ward LM, Pace LA, Fischer WW. 2015. Draft genome sequence of Ardenticatena maritima 110S, a thermophilic nitrate- and iron-reducing member of the Chloroflexi class Ardenticatenia. Genome Announc 3(6):e01347-15.

33. HILL, M.O., 1973, Diversity and evenness: a unifying notation and its consequences: Ecology, v. 54, p. 427–432.

34. Hirayama, Hisako, et al. "Methylomarinovum caldicuralii gen. nov., sp. nov., a moderately thermophilic methanotroph isolated from a shallow submarine hydrothermal system, and proposal of the family Methylothermaceae fam. nov." *International journal of systematic and evolutionary microbiology* 64.3 (2014): 989-999.

35. Holland HD (1984) The chemical evolution of the atmosphere and oceans. Princeton University Press.

36. Hurowitz, Joel A., et al. "Origin of acidic surface waters and the evolution of atmospheric chemistry on early Mars." *Nature Geoscience* 3.5 (2010): 323-326.

37. Imhoff, Johannes F. "The Family Chromatiaceae." *The Prokaryotes*. Springer Berlin Heidelberg, 2014. 151-178.

38. Johnson, J. E., Gerpheide, A., Lamb, M. P. & Fischer, W. W. O2 constraints from Paleoproterozoic detrital pyrite and uraninite. *Geol. Soc. Am. Bull.* **126,** 813–830 (2014).

39. Johnston, David T., et al. "Anoxygenic photosynthesis modulated Proterozoic oxygen and sustained Earth's middle age." *Proceedings of the National Academy of Sciences* 106.40 (2009): 16925-16929.

40. Kale, V. et al. Litorilinea aerophila gen. nov., sp. nov., an aerobic member of the class Caldilineae, phylum Chloroflexi, isolated from an intertidal hot spring. Int. J. Syst. Evol. Microbiol. 63, 1149–1154 (2013).

41. Kaneoka, Ichiro, Naoki Isshiki, and Shigeo Zashu. "K-Ar ages of the Izu-Bonin islands." *Geochemical Journal* 4.2 (1970): 53-60.

42. Kasting, James F. "What caused the rise of atmospheric O 2?." *Chemical Geology* 362 (2013): 13-25.

43. Kato, S. *et al.* Comparative genomic insights into ecophysiology of neutrophilic, microaerophilic iron oxidizing bacteria. *Front. Microbiol.* **6,** 1–16 (2015).

44. Katoh, Kazutaka, et al. "MAFFT: a novel method for rapid multiple sequence alignment based on fast Fourier transform." Nucleic acids research 30.14 (2002): 3059-3066.

45. Kharecha, P., Kasting, J. & Siefert, J. A coupled atmosphere–ecosystem model of the early Archean Earth. *Geobiology* **3,** 53–76 (2005).

46. Kielak, Anna M., et al. "The ecology of Acidobacteria: moving beyond genes and genomes." *Frontiers in Microbiology* 7 (2016).

47. Klatt, C. G. et al. Community ecology of hot spring cyanobacterial mats: predominant populations and their functional potential. ISME J. 5, 1262–1278 (2011).

48. Klueglein, N., and A. Kappler. Abiotic oxidation of Fe (II) by reactive nitrogen species in cultures of the nitrate-reducng Fe(II) oxidizer Acidovorax sp. BoFeN1— questioning the existence of enzymatic Fe(II) oxidation. Geobiology 11.2 (2013): 180-190.

49. Konhauser, K. O. *et al*. Could bacteria have formed the Precambrian banded iron formations? *Geology* **30,** 1079–1082 (2002).

50. Krepski, S. T., Emerson, D., Hredzak-Showalter, P. L., Luther III, G. W. & Chan, C. S. Morphology of biogenic iron oxides records microbial physiology and environmental conditions: toward interpreting iron microfossils. *Geobiology* **11,** 457–471 (2013).

51. Lebedeva EV, Off S, Zumbragel S, Kruse M, Shagzhina A, Lucker S, Maixner F, Lipski A, Daims H, Spieck E (2011) Isolation and characterization of a moderately thermophilic nitrite-oxidizing bacterium from a geothermal spring. FEMS Microbiol

Ecol 75:195–204

52. Li H.*, Handsaker B.*, Wysoker A., Fennell T., Ruan J., Homer N., Marth G., Abecasis G., Durbin R. and 1000 Genome Project Data Processing Subgroup (2009) The Sequence alignment/map (SAM) format and SAMtools. Bioinformatics, 25, 2078-9. [PMID: 19505943]

53. LOZUPONE, C., AND KNIGHT, R., 2005, UniFrac: a new phylogenetic method for comparing microbial communities: Applied and Environmental Microbiology, v. 71, p. 8228–8235.

54. McIlroy, Simon Jon, and Per Halkjær Nielsen. "The family saprospiraceae." *The Prokaryotes*. Springer Berlin Heidelberg, 2014. 863-889.

55. Meyer-Dombard, D., Jan P. Amend, and Magdalena R. Osburn. "Microbial diversity and potential for arsenic and iron biogeochemical cycling at an arsenic rich, shallow-sea hydrothermal vent (Tutum Bay, Papua New Guinea)." Chemical Geology 348 (2013): 37-47.

56. Miller, M.A., Pfeiffer, W., and Schwartz, T. (2010) "Creating the CIPRES Science Gateway for inference of large phylogenetic trees" in Proceedings of the Gateway Computing Environments Workshop (GCE), 14 Nov. 2010, New Orleans, LA pp 1 - 8.

57. Neubauer, S. C. et al. Life at the energetic edge: kinetics of circumneutral Fe oxidation by lithotrophic iron oxidizing bacteria isolated from the wetland plant rhizosphere. Appl. Environ. Microbiol. 68, 3988–3995 (2002).

58. Oksanen, Jar, F. Guillaume Blanchet, Roeland Kindt, Pierre Legendre, Peter R. Minchin, R. B. O'Hara, Gavin L. Simpson, Peter Solymos, M. Henry H. Stevens and Helene Wagner (2016). vegan: Community Ecology Package. R package version 2.3-5. https://CRAN.R-project.org/package=vegan

59. Pace LA, Hemp J, Ward LM, Fischer WW. 2015. Draft genome of Thermanaerothrix daxensis GNS-1, a thermophilic facultative anaerobe from the Chloroflexi class Anaerolineae. Genome Announc 3(6):e01354-15.

60. PARADA, A., NEEDHAM, D.M., AND FUHRMAN, J.A., 2015, Every base matters: assessing small subunit rRNA primers for marine microbiomes with mock communities, time-series and global field samples: Environmental Microbiology, v. 18, p. 1403–1414.

61. Pester, Michael, Christa Schleper, and Michael Wagner. "The Thaumarchaeota: an emerging view of their phylogeny and ecophysiology." *Current opinion in microbiology* 14.3 (2011): 300-306.

62. Pierson, B. K., Paranteau, M. N. & Griffin, B. M. Phototrophs in high-iron-concentration microbialmats: Physiological ecology of phototrophs in an iron-depositing hot spring. Appl. Environ.Microbiol. 65, 5474–5483 (1999). 36.

63. Poulton, Simon W., Philip W. Fralick, and Donald E. Canfield. "Spatial variability in oceanic redox structure 1.8 billion years ago." *Nature Geoscience* 3.7 (2010): 486-490.

64. Price MN, Dehal PS, Arkin AP. 2010. FastTree 2-Approximately Maximum-Likelihood Trees for Large Alignments. Plos One 5(3).

65. Pujalte, María J., et al. "The family Rhodobacteraceae." *The Prokaryotes: Alphaproteobacteria and Betaproteobacteria* (2014): 439-512.

66. Quast, Christian, et al. "The SILVA ribosomal RNA gene database project: improved data processing and web-based tools." Nucleic acids research41.D1 (2013): D590-D596.

67. R Core Team. 2014. R: A language and environment for statistical computing. R Foundation for Statistical Computing, Vienna, Austria.

68. Rantamäki, S. et al. Oxygen produced by cyanobacteria in simulated Archaean conditions partly oxidizes ferrous iron but mostly escapes—conclusions about early evolution. Photosynth. Res. 1–9 (2016).

69. Rodrigues, Jorge LM, and Jantiya Isanapong. "The family Opitutaceae." *The Prokaryotes*. Springer Berlin Heidelberg, 2014. 751-756.

70. Roeselers, G. et al. Diversity of phototrophic bacteria in microbial mats from Arctic hot springs (Greenland). Environ. Microbiol. 9, 26–38 (2007).

71. Rosenberg, Eugene. "The family Chitinophagaceae." *The Prokaryotes*. Springer Berlin Heidelberg, 2014. 493-495.

72. Sahoo SK, et al. (2012) Ocean oxygenation in the wake of the Marinoan glaciation. Nature 489(7417):546–549.

73. Scott, C., et al. "Tracing the stepwise oxygenation of the Proterozoic ocean." *Nature* 452.7186 (2008): 456-459.

74. Sekiguchi, Y. et al. Anaerolinea thermophila gen. nov., sp. nov. and Caldilinea aerophila gen. nov., sp. nov., novel filamentous thermophiles that represent a

previously uncultured lineage of the domain Bacteria at the subphylum level. Int. J. Syst. Evol. Microbiol. 53, 1843–1851 (2003).

75. Shannon, C. E. (1948) A mathematical theory of communication. The Bell System Technical Journal, 27, 379–423 and 623–656.

76. Shih, P. M. & Matzke, N. J. Primary endosymbiosis events date to the later Proterozoic with cross-calibrated phylogenetic dating of duplicated ATPase proteins. *Proc. Natl. Acad. Sci. U. S. A.* **110,** 12355–60 (2013).

77. Shih, P., Hemp, J., Ward, L., Matzke, N. & Fischer, W. 2016. Crown group oxyphotobacteria postdate the rise of oxygen. Geobiology.

78. SIMPSON, E.H., 1949, Measurement of diversity: Nature, v. 163, p. 688.

79. Skennerton, C. T. *et al.* Genomic reconstruction of an uncultured hydrothermal vent gammaproteobacterial methanotroph (family Methylothermaceae) indicates multiple adaptations to oxygen limitation. *Front. Microbiol.* **6,** 1–12 (2015).

80. A. Stamatakis: "RAxML Version 8: A tool for Phylogenetic Analysis and Post-Analysis of Large Phylogenies". In Bioinformatics, 2014

81. Stamenković V, LM Ward, and WW Fischer. 2017. Supercool oxygen Oases on Mars. In prep.

82. Stookey, Lawrence L. "Ferrozine---a new spectrophotometric reagent for iron." Analytical chemistry 42.7 (1970): 779-781.

83. Swanner, E. D. et al. Modulation of oxygen production in Archaean oceans by episodes of Fe(II) toxicity. Nat. Geosci. 8, 126–130 (2015).

84. Takai, Ken, and Satoshi Nakagawa. "The Family Hydrogenothermaceae."The
    Prokaryotes. Springer Berlin Heidelberg, 2014. 689-699.

85. Trembath-Reichert E, Ward LM, Slotznick SP, Bachtel SL, Kerans C, Grotzinger JP,
    Fischer WW (2016) Gene sequencing microbial community analysis of mat
    morphologies, Caicos Platform, British West Indies, Journal of Sedimentary
    Research.

86. Walker, J. C. & Brimblecombe, P. Iron and sulfur in the pre-biologic ocean.
    Precambrian Res. **28,** 205–222 (1985).

87. Wang Q, Garrity GM, Tiedje JM, Cole JR. 2007. Naive Bayesian classifier for rapid
    assignment of rRNA sequences into the new bacterial taxonomy. Appl Environ
    Microb 73(16): 5261-5267.

88. Ward LM, Hemp J, Pace LA, Fischer WW. 2015. Draft genome sequence of Leptolinea
    tardivitalis YMTK-2, a mesophilic anaerobe from the Chloroflexi class Anaerolineae.
    Genome Announc 3(6):e01356-15.

89. Ward, L. M., Kirschvink, J. L. & Fischer, W. W. 2016. Timescales of Oxygenation
    Following the Evolution of Oxygenic Photosynthesis. Orig. Life Evol. Biosph. 46(1)
    pp51-65.

90. Ward LM, A Idai, T Kakegawa, WW Fischer, and SE McGlynn. 2017. Microbial
    diversity and iron oxidation at Okuoku-hachikurou Onsen, a Japanese hot spring analog
    of Precambrian iron formation. Geobiology, in revision.

91. Waterhouse, A.M., Procter, J.B., Martin, D.M.A, Clamp, M. and Barton, G. J. (2009) "Jalview Version 2 - a multiple sequence alignment editor and analysis workbench" Bioinformatics25 (9) 1189-1191 doi: 10.1093/bioinformatics/btp033

92. H. Wickham. ggplot2: Elegant Graphics for Data Analysis. Springer-Verlag New York, 2009.

93. Yamada, T. et al. Anaerolinea thermolimosa sp. nov., Levilinea saccharolytica gen. nov., sp. nov. and Leptolinea tardivitalis gen. nov., sp. nov., novel filamentous anaerobes, and description of the new classes Anaerolineae classis nov. and Caldilineae classis nov. in the. Int. J. Syst. Evol. Microbiol. 56, 1331–1340 (2006).

94. Yoon, J., Jang, J. H. & Kasai, H. Algisphaera agarilytica gen nov, sp nov, a novel representative of the class Phycisphaerae within the phylum Planctomycetes isolated from a marine alga. *Antonie van Leeuwenhoek, Int. J. Gen. Mol. Microbiol.* **105,** 317–324 (2014)

95. Youssef, N. H. *et al.* In Silico Analysis of the Metabolic Potential and Niche Specialization of Candidate Phylum 'Latescibacteria' (WS3). *PLoS One* **10,** e0127499 (2015).

96. Zerkle, A. L. *et al.* Onset of the aerobic nitrogen cycle during the Great Oxidation Event. *Nature* 1–10 (2017). doi:10.1038/nature20826